*sustainability*

*Article*

# Determination of the Processing Route for Obtaining Calcium Acetate from Eggshell Waste

**Jasmine Keise de Oliveira Silva [1,2], Carla Bittencourt [3], Alexandre Zirpoli Simões [2] and Ana Paula Rosifini Alves [1,2,*]**

[1] School of Engineering, São Paulo State University (UNESP), Ilha Solteira 15385-007, Brazil; jasmine.keise@unesp.br
[2] School of Engineering and Sciences, São Paulo State University (UNESP), Guaratinguetá 12516-410, Brazil; zirpoli.simoes@unesp.br
[3] Research Institute for Materials Science and Engineering, University of Mons (UMONS), Avenue Copernic 3, 7000 Mons, Belgium; carla.bittencourt@umons.ac.be
* Correspondence: paula.rosifini@unesp.br

## Abstract

Eggshell waste represents an underutilized biogenic resource, rich in calcium carbonate and organic components, whose increasing generation poses significant environmental and economic challenges. It is estimated that more than 8 million tons of eggshells are produced worldwide annually, most of which are disposed of in landfills, leading to landfill overload and increased waste management costs. In this context, the main objective of this study was to develop and compare three processing routes for converting calcium carbonate derived from eggshell waste into calcium acetate, using commercial vinegar (4–5% acetic acid) as a low-cost, sustainable acid source. The proposed routes were systematically evaluated based on processing efficiency, product characteristics, and operational simplicity. The materials obtained were characterized by X-ray fluorescence, scanning electron microscopy (SEM), energy-dispersive X-ray spectroscopy (EDS), X-ray diffraction (XRD), Fourier-transform infrared spectroscopy (FTIR), thermogravimetric analysis (TGA/DTG), X-ray photoelectron spectroscopy (XPS), particle size analysis, and zeta potential measurements. The results indicated that the eggshells contained approximately 95.39% calcium, confirming their suitability as an efficient calcium precursor. Among the routes evaluated, the process using a spherical condenser under reflux at 90 °C showed superior performance, achieving shorter reaction times and maintaining comparable yields of membrane byproducts compared to the other methods. This approach differs from conventional routes by eliminating the need for high-purity reagents, reducing processing time, and using exclusively food-grade acetic acid, thus increasing sustainability and cost-effectiveness. Morphological, chemical, and thermal analyses confirmed the quality and stability of the synthesized calcium acetate. In general, these results demonstrate that eggshell waste can be efficiently valorized into calcium acetate through a scalable, straightforward process, thereby reducing landfill disposal and supporting circular economy strategies, with potential applications in the production of calcium-based biomaterials.

**Keywords:** eggshell waste; calcium acetate; biomaterials; sustainable

Academic Editors: Simeng Li and Tolulope A. Agunbiade

Received: 27 November 2025
Revised: 22 January 2026
Accepted: 23 January 2026
Published: 1 February 2026

## 1. Introduction

Over the past 30 years, global egg production has increased by around 150%, leading to a significant rise in eggshell waste. Asia, the primary hub for egg production, accounts

https://doi.org/10.3390/su18031448

for more than 64% of the world's total production. This concentration creates significant environmental, economic, and biological challenges related to the accumulation and disposal of eggshells [1]. When improperly managed, this biogenic waste contributes to landfill overload and poses health risks, underscoring the urgent need for sustainable recovery strategies.

The disposal of eggshells has attracted growing attention as a promising and sustainable source for the production of calcium-based bioceramics, owing to their intrinsic chemical composition and hierarchical structure, which are favorable for biomaterial applications [2]. Poultry eggshells are composed mainly of calcium carbonate ($CaCO_3$), accounting for about 96% by weight, with the remaining fraction consisting of an organic membrane and trace elements such as magnesium, phosphorus, and sodium [3]. These intrinsic properties, independent of economic factors, make eggshells particularly suitable for conversion into high-value-added calcium precursors. In addition, their wide availability and low cost further increase their attractiveness as a raw material from a sustainability perspective [4].

In bone regeneration and tissue engineering, bioactive inorganic materials—including hydroxyapatite, β-tricalcium phosphate, tetracalcium phosphate, and dicalcium phosphate—are widely incorporated into structures to enhance bioactivity, biocompatibility, and osteoconductive or osteoinductive properties. The synthesis of these materials often requires high-purity calcium precursors, which significantly increase production costs and limit scalability. In this regard, calcium sources derived from eggshell waste—readily available from domestic, commercial, and agricultural sources—offer an economically and environmentally appealing alternative to synthetic reagents [5,6].

Numerous processing methods [7–13] have been researched to convert eggshells into calcium-based precursors, such as calcium carbonate ($CaCO_3$), calcium oxide (CaO), and calcium acetate ($Ca(CH_3COO)_2$). These methodologies exploit the high calcium carbonate content of eggshells and their abundance as agro-industrial waste, making them a valuable raw material for biomedical, environmental, and industrial applications.

Among these methods, calcium carbonate nanostructures derived from eggshells have gained significant attention due to their high biocompatibility and chemical similarity to natural bone tissue. Tavangar et al. [7] reported the synthesis of three-dimensional nanofibrous $CaCO_3$ structures using femtosecond laser ablation, which does not require additional chemical reagents. In this process, ultrafast laser pulses induce localized vaporization and reorganization of the calcium carbonate in the eggshell, resulting in an interconnected network of nanofibers with diameters in the tens of nanometers. The authors demonstrated that adjusting the laser parameters can control the final morphology of the structures. They emphasized the high potential of these nanofibers for tissue engineering applications, though the process requires expensive equipment and consumes substantial energy.

Torres-Mansilla et al. [8] investigated the hydrothermal transformation of calcium carbonate derived from eggshells into micro- and nanoparticle apatite using phosphate solutions under controlled temperature and pressure conditions. This process was conducted in a hydrothermal autoclave at temperatures ranging from 120 °C to 200 °C, facilitating the gradual conversion of carbonate into crystalline apatite. The resulting materials exhibited adjustable morphologies, high cytocompatibility, and superior osteoinductive properties, as evidenced by in vitro tests with osteoblastic cells. However, the authors caution that the reliance on pressurized systems and high temperatures may limit the industrial scalability of this method.

In contrast, the reaction between calcium carbonate from eggshells and acetic acid has become a mild synthetic method for producing calcium acetate, a highly soluble organic salt commonly used as a precursor in biomedical, pharmaceutical, and industrial applications. Studies show that this reaction can be carried out at moderate temperatures, using simple equipment and achieving high chemical yield [13–19].

Strelec et al. [17] reported the production of high-purity calcium acetate monohydrate from eggshells using diluted acetic acid solutions, achieving yields exceeding 75%. The study also highlighted the possibility of simultaneously recovering the shell membranes, adding value to the process from a circular-economy perspective. Similarly, Yao et al. [18] applied response surface methodology (RSM) to optimize reaction parameters, including acid concentration, solid-to-liquid ratio, and temperature, achieving yields greater than 90% under the optimized conditions.

Research conducted by Menglieva et al. [19] has demonstrated that calcium acetate can be synthesized from eggshells using environmentally friendly methods. These methods require low energy consumption and do not necessitate high-purity reagents, indicating that this approach has significant potential for large-scale applications. Despite these advances, most available studies focus on specific processing conditions and lack systematic comparisons across different reaction configurations, such as open systems, reflux, or assisted extraction.

Although the number of studies on the valorization of eggshells has been growing significantly, comparative analyses that simultaneously evaluate efficiency, scalability, operational simplicity, and final product quality for calcium acetate production are still limited. Recent reviews highlight the need for studies that critically compare different synthesis routes, accounting for parameters such as energy consumption, reagent accessibility, and the physicochemical properties of the resulting material [16,20–22].

In this context, this study proposes the development and comparison of three simple and technically feasible synthesis routes—open system, Soxhlet-assisted system, and spherical condenser system—for the production of calcium acetate from eggshell waste. A key difference in this work is the use of commercial food-grade vinegar as an alternative source of acetic acid, thereby reducing costs and increasing the process's sustainability. The systematic comparison of different routes based on yield, chemical purity, particle characteristics, and operational feasibility is intended to identify an efficient, scalable method for converting eggshell waste into calcium acetate. This advancement has potential applications in biomaterials, bone regeneration, and tissue engineering, as well as contributing to circular economy strategies.

## 2. Materials and Methods

The flowchart in Figure 1 illustrates the experimental procedures performed in this study. Initially, raw eggshells were collected from households, washed with running water, air-dried, and stored in plastic containers. According to the methodology reported by Strelec et al. [23], approximately 30 g of pre-cleaned eggshells were subjected to an additional washing step consisting of three cycles of 30 min each in 300 mL of deionized water, using an orbital shaker operated at 250 rpm at room temperature. This repeated washing protocol was adopted to ensure the effective removal of residual organic matter, soluble proteins, and weakly bound impurities originating from the eggshell membrane and surface contaminants. Such contaminants can interfere with subsequent chemical reactions and compromise the purity of calcium-based products. The use of multiple washing cycles rather than a single-step wash has been shown to improve the chemical homogeneity and reproducibility of eggshell-derived precursors, thereby contributing to greater product purity; however, no direct comparison with simplified washing procedures was performed in this study. After washing, the eggshells were dried in an oven at 50 °C for 24 h [23].

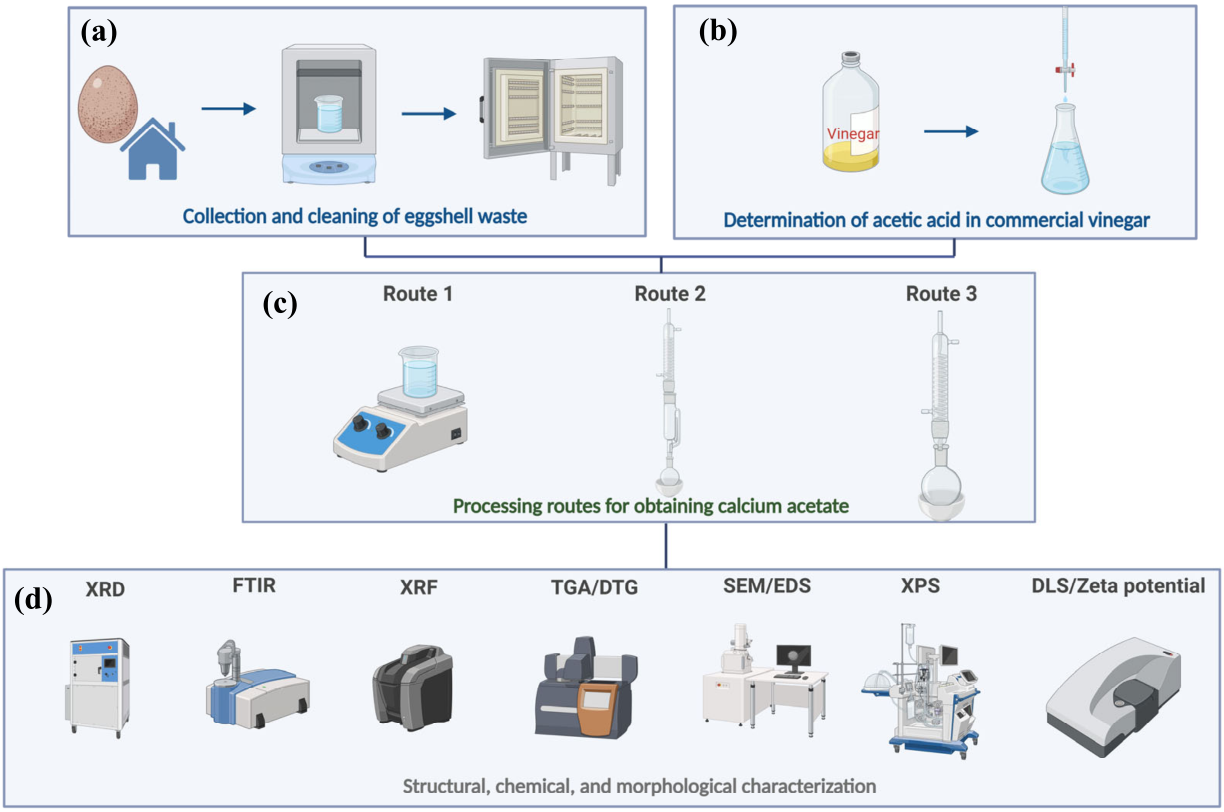

**Figure 1.** Flowchart of the methodology used (**a**) Collection and cleaning of eggshell waste, (**b**) Determination of acetic acid in commercial vinegar, (**c**) Processing routes for obtaining calcium acetates, and (**d**) Characterization techniques performed.

The acetic acid concentration in commercial vinegar was measured using potentiometric titration. Conductometric titration served as an independent validation method for these measurements. By employing both techniques, we ensured the reliability and accuracy of the acid concentration values that were used in the stoichiometric calculations for the subsequent synthesis reactions.

Initially, a 0.10 M NaOH solution (≥97% purity, Synth, Diadema, Brazil) was prepared and standardized against potassium acid phthalate (≥99% purity, Êxodo Scientific, Sumaré, Brazil). Three drops of phenolphthalein indicator (≥99% purity, Neon Comercial Ltda., Suzano, Brazil) were added, and the solution was titrated until the appearance of a persistent pale pink endpoint. The standardization procedure was performed in triplicate to assess reproducibility, and the molar concentration of NaOH showed a relative standard deviation of 1.8%, indicating good repeatability.

To determine the acetic acid content in commercial vinegar, a 3 mL aliquot of vinegar was diluted in 40 mL of deionized water using a graduated pipette, followed by the addition of three drops of phenolphthalein indicator. Titration was carried out using the previously standardized NaOH solution. This initial titration was performed once to establish the approximate equivalence point and define the titration range for instrumental measurements.

Subsequently, potentiometric titration was conducted under the same conditions by coupling a pH electrode to the titration system. The pH was recorded after each incremental addition of 0.10 M NaOH. The analytical concentration of acetic acid was determined from plots of pH versus titrant volume and from the first derivative of the titration curve. Using this method, an acetic acid concentration of 4.14% was obtained.

To validate the potentiometric results and provide an independent confirmation of the equivalence point, conductometric titration was also performed. The NaOH solution used as titrant was standardized again in triplicate before this analysis. During the titration, 1 mL aliquots of 0.10 M NaOH were added to a total solution volume of 40 mL, and the electrical conductivity was recorded after each addition. The equivalence point was determined from the conductance-versus-titrant-volume plot. This method yielded an acetic acid concentration of 4.45%, which is in good agreement with the value obtained by potentiometric titration, confirming the reliability of the measurements.

### 2.1. Synthesis of Calcium Acetate

The chemical transformation of calcium carbonate in eggshell into calcium acetate, using commercial vinegar, is described in Equation (1). The appropriate calculations were performed for 500 mL of vinegar, using the percentage of acetic acid determined by titration.

$$CaCO_3(s) + 2CH_3COOH(aq) \rightarrow C_4H_6CaO_4(aq) + H_2O(l) + CO_2(g) \quad (1)$$

To ensure that there is an excess of acetic acid and that the chemical transformation takes place completely, 40% less of the eggshell mass calculated for the 1:2 ratio of $CaCO_3$ to $CH_3COOH$ was considered beforehand.

To optimize the process time, three distinct synthesis routes were evaluated, as shown in Figure 2.

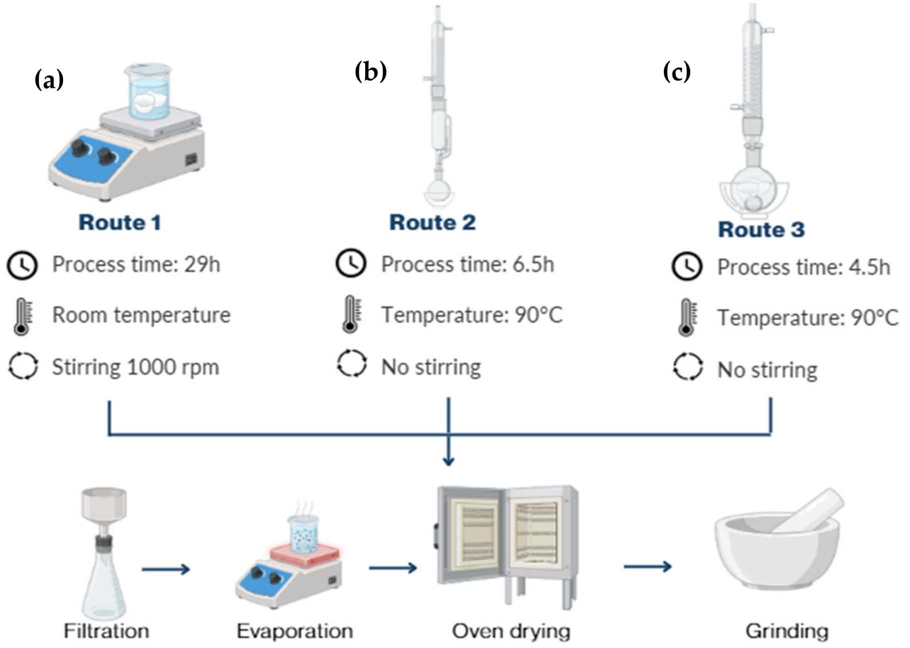

**Figure 2.** Illustration of the three routes for synthesizing calcium acetate from eggshell waste. (**a**) Route 1: 29 h, room temperature, stirring at 1000 rpm. (**b**) Route 2: 6.5 h, 90 °C, no stirring. (**c**) Route 3: 4.5 h, 90 °C, no stirring.

### 2.2. Route 1: Open System

A system was set up as illustrated in Figure 2a. Pieces of eggshell were mixed in 500 mL of commercial vinegar in a beaker under a magnetic stirrer at 1000 rpm. It took about 29 h for the eggshell to be entirely consumed by the vinegar, obtaining the membrane as a by-product.

### 2.3. Route 2: Soxhlet Extractor

To reduce the time required for the chemical transformation process, a Soxhlet extractor (Plena-Lab Indústria e Comércio Ltda., São Paulo, Brazil) was used in conjunction with a volumetric flask, both of which were placed under a heating mantle at 90 °C. Pieces of eggshell were placed in the extractor compartment, and 500 mL of vinegar was added to the volumetric flask (Figure 2b). In this procedure, when the solvent (vinegar) is heated, reflux occurs due to the condenser as the steam rises into the flask and condenses in the central part of the Soxhlet. With each cycle, the eggshell dissolves in the acetic acid vapor. Complete dissolution occurred in 6 h, producing membranes as a by-product, similar to route 1.

### *2.4. Route 3: Ball Condenser*

The route is shown in Figure 2c was also used, consisting of a ball condenser and a volumetric flask containing the solvent (vinegar) and the eggshell sample. The entire apparatus was placed under a heating blanket at 90 °C. The chemical transformation process using this procedure took 4.5 h, and membranes were obtained as a by-product.

The three routes yielded calcium acetate solutions and membranes as by-products, which were subsequently separated by a filtration step. The calcium acetate solutions obtained were evaporated to obtain the calcium acetate precipitate. The membranes obtained from the three routes were washed three times in an orbital shaker at 250 rpm for 15 min each in deionized water, followed by a 10 min wash in acetone, and then dried in an oven at 60 °C for 24 h. The membranes were stored in plastic containers for analysis.

### *2.5. Characterization*

The analysis of the crystalline phases present in the eggshell and calcium acetate powder samples was performed by means of X-ray diffraction. The equipment used for the analyses was the Bruker D8 Advance diffractometer (Bruker AXS GmbH, Karlsruhe, Germany). Cu K$\alpha$ radiation (0.15418 nm), 25 mA current, and 40 kV voltage were used for the study, with a 2$\theta$ measurement interval of 5° to 90°, 0.02° step, and 0.35 s counting time.

A Perkin-Elmer Spectrum System 100 ATR FTIR spectrophotometer (PerkinElmer Inc., Waltham, MA, USA) was used to perform Fourier-transform infrared spectroscopy (FTIR) to evaluate the functional groups present in the eggshell, membrane, and calcium acetate samples obtained by the three routes.

The chemical composition of the eggshell and calcium acetate sample, resulting from the evaporation of solutions obtained from the three configurations and varying the mass of the eggshell, was evaluated by X-ray fluorescence using an Axios Max-PANalytical wavelength dispersive XRF spectrometer (PANalytical B.V., Almelo, The Netherlands).

The behavior of eggshell and calcium acetate samples as a function of temperature, in an environment with controlled temperature and atmosphere, was evaluated by means of thermogravimetric analysis, using the SII Nanotechnology-Seiki equipment, model TG/DTA 6200 (SII NanoTechnology Inc., Tokyo, Japan). The parameters used to perform this technique were: 10 mg of sample, platinum sample holder, inert nitrogen atmosphere with a flow rate of 100 mL/min, temperature range of 40 to 1000 °C, and alumina reference material.

The morphology of the eggshell and calcium acetate powders obtained from this waste, was evaluate by scanning electron microscopy EVO LS15-Zeiss (Carl Zeiss Microscopy GmbH, Oberkochen, Germany). A small number of samples were placed on aluminum support using double-sided carbon tape. The samples were then coated with a thin layer of gold and analyzed under high vacuum. The eggshell and calcium acetate samples were also analyzed semi-quantitatively by energy-dispersive spectrometry (EDS) using an Oxford Instruments spectrometer (Oxford Instruments plc, Abingdon, UK) at 20.0 keV.

The particle size, zeta potential, and molecular weight of calcium acetate particles stably dispersed in a liquid medium (deionized water) were measured using a Zetasizer

Nano ZS, model ZEN 3601 (Malvern Instruments Ltd., Malvern, UK). All measurements were performed in triplicate.

The eggshell and calcium acetate samples obtained by the three routes were analyzed by X-ray photoelectron spectroscopy using a PHI Genesis instrument from Physical Electronics (Chanhassen, MN, USA), equipped with a monochromatic Al K$\alpha$ X-ray source, operating at 48.7 W. The pressure in the analysis chamber was $10^{-9}$ mbar, the passage energy was 27 eV, and the analysis area was 200 × 200 microns. The fitting analysis was performed using CASAXPS (Version 2.3.26), with Gauss-Lorentz convolution to analyze the components and the Shirley background. The Gaussian component accounts for instrumental broadening, while the Lorentzian component represents the intrinsic lifetime broadening of the core-level electrons. The convolution of these functions allows for a more accurate representation of the experimental peak shapes and enables reliable deconvolution of overlapping chemical states.

## 3. Results

Figure 3 shows the final products obtained from the synthesis routes employed to convert the calcium carbonate present in eggshells into calcium acetate. Both processes produced white powders with a similar appearance. Similar results were reported by Strelec et al. [17] and Yao et al. [18], who obtained calcium acetate from eggshells using acetic acid, yielding a homogeneous white powder after evaporation and drying.

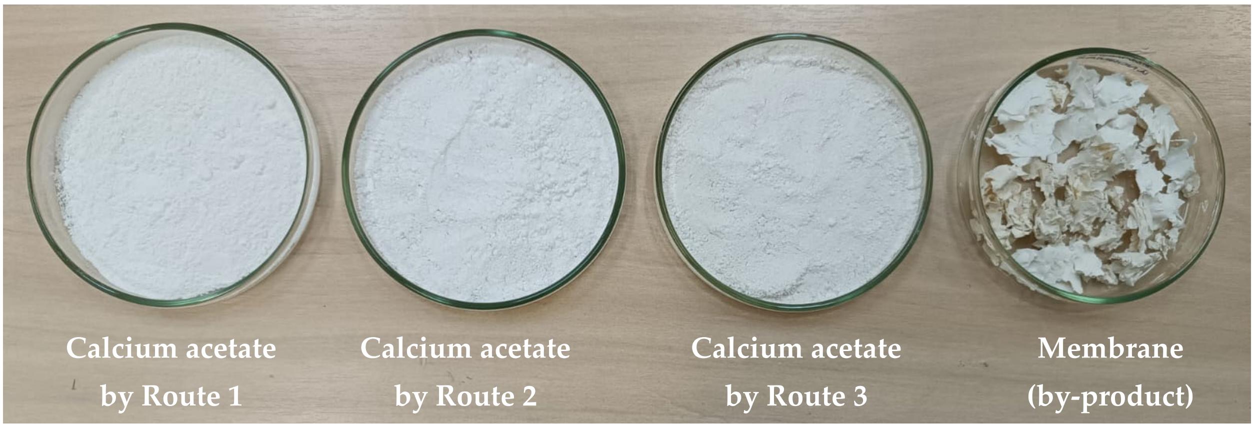

**Figure 3.** Calcium acetate products obtained from the three synthesis routes, with eggshell membrane recovered as a by-product.

In addition, the residual shell membrane was fully recovered during processing and can be reused in biomedical applications, highlighting the methodology's sustainability [23,24]. Table 1 summarizes the processing time and yields of the byproducts obtained. Route 3 had the shortest processing time, and membrane yield was similar across all methods. This behavior can be attributed to the higher heat transfer efficiency and improved recovery of acetic acid vapors enabled by the spherical condenser, which favors the kinetics of the acid-base reaction. In contrast, studies such as that of Yao et al. [18] report longer processing times, mainly when the reaction is carried out in conventional systems without efficient reflux, even under optimized concentration and temperature conditions. Despite differences in processing time, membrane yield remained similar across all routes, indicating that membrane integrity was not significantly affected by the experimental set up.

**Table 1.** Processing time for calcium acetate and byproduct (membrane) yield for the three methods used.

| Route | Process Time (h) | Membrane Yield (%) | Average Standard Deviation of Membrane Yield (%) |
|---|---|---|---|
| 1 | 29 | 3.12 | 0.28 |
| 2 | 6.5 | 3.08 | 0.36 |
| 3 | 4.5 | 3.17 | 0.31 |

The average zeta potential of the commercial calcium acetate sample and those obtained by the three processing routes can be observed in Figure 4. The samples exhibit a negative charge, with values between −11.167 and −0.462 mV, indicating colloidal instability with a high tendency to aggregate or low stability [25,26]. Such behavior may limit their direct use in biomedical applications, as particle aggregation can adversely affect suspension homogeneity, injectability, cellular interaction, and ion release kinetics. Previous studies have shown that colloidal instability in calcium-based materials can compromise biological performance and reproducibility in biomedical systems [27,28]. Therefore, additional stabilization strategies—such as surface functionalization, pH control, or the use of dispersing and stabilizing agents—are often required to improve colloidal stability and ensure suitability for biomedical applications [29,30].

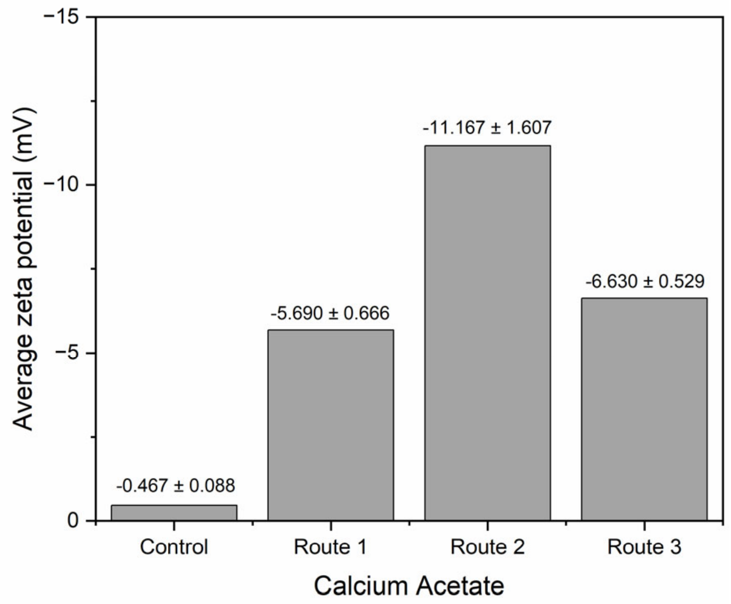

**Figure 4.** Average zeta potential of the samples.

Table 2 presents the average particle sizes obtained by dynamic light scattering (DLS) for the analyzed samples, corresponding to the hydrodynamic diameters of the particles in suspension, including not only the solid core but also the solvation layer and possible agglomerates formed in the dispersing medium [25,26]. The average Z-value of the control sample (1230 nm) indicates the presence of relatively large particles, consistent with the tendency of calcium-based materials to aggregate in aqueous media due to electrostatic interactions and Van der Waals forces [27,28].

**Table 2.** Particle size by DLS of calcium acetate samples.

| Calcium Acetate | Z Average (d.nm) | Standard Deviation (d.nm) | PdI | Standard Deviation PdI |
|---|---|---|---|---|
| Control | 1230.67 | 77.11 | 0.094 | 0.109 |
| Route 1 | 2461.67 | 104.22 | 0.190 | 0.161 |
| Route 2 | 2775.67 | 342.78 | 0.184 | 0.159 |
| Route 3 | 2266.67 | 169.56 | 0.292 | 0.105 |

In comparison, the samples obtained by the three processing routes (2266–2775 nm) show a significant increase in average particle size, suggesting a greater tendency toward agglomeration induced by synthesis conditions, such as temperature, reaction time, and mixing regime. According to Bhattacharjee [26], variations in chemical and thermal processing can intensify particle collisions, favoring the formation of agglomerates detectable by DLS, such as an increase in hydrodynamic diameter.

Among the evaluated routes, the sample obtained from Route 2 has the highest average Z value, indicating that the employed processing method intensifies interparticle interactions, increasing the probability of forming larger agglomerates. This behavior is consistent with studies that demonstrate that systems with longer residence times or less efficient dispersion conditions tend to exhibit greater aggregation in calcium-based materials [27,29]. In contrast, the samples produced by Routes 1 and 3 exhibit slightly smaller average sizes than those from Route 2, suggesting a lower degree of agglomeration.

Notably, the sample obtained by Route 3 has the smallest average particle size among all synthesized samples, indicating that this processing configuration favors better particle dispersion and reduces agglomeration formation. Similar results were reported by Vo et al. [27], who observed synthesis routes that minimize aggregation yield particles with more stable colloidal behavior, which is particularly relevant for biomedical applications.

The polydispersity index (PDI) provides additional information on the uniformity of the particle size distribution. The control sample has a PDI of less than 0.1, indicating a narrow size distribution and an essentially monodisperse system, as defined by widely accepted criteria in the literature [25,26]. In contrast, the samples produced by Routes 1, 2, and 3 exhibit PDI values between 0.1 and 0.3, indicating moderately dispersed systems with some particle-size heterogeneity.

According to Honary and Zahir [25] and Dorozhkin [28], PDI values below 0.3 are still considered acceptable for colloidal suspensions intended for biomedical applications, indicating relative stability of the system. Consequently, the PDI results support the DLS measurements and confirm that the processing routes significantly affect agglomeration behavior and particle size distribution, with Route 3 providing the best balance between dispersion and uniformity.

The crystalline phases present in the samples of raw eggshell and calcium acetate powder obtained by different synthesis routes were investigated by X-ray diffraction (XRD), as illustrated in Figure 5. XRD analysis was used to identify the phases present, evaluate the crystalline purity of the products formed, and verify possible structural transformations resulting from chemical processing.

The diffractogram of the eggshell sample showed well-defined, intense diffraction peaks characteristic of the calcite phase ($CaCO_3$), indicating high crystallinity of the material. The prominent peaks were observed in the crystallographic planes (012), (104), (110), (113), (202), and (024), corresponding to the values of $2\theta = 23.109°$, $29.547°$, $36.107°$, $39.459°$, $43.219°$, and $47.592°$, respectively. These $2\theta$ values and the relative peak intensities are in excellent agreement with data reported for calcite on standard crystallographic bases, confirming that the calcium carbonate present in eggshell is predominantly in this crystalline phase. Similar results were reported by May Yu et al. [31], who also identified calcite as the primary phase in eggshell residues intended for the synthesis of calcium salts.

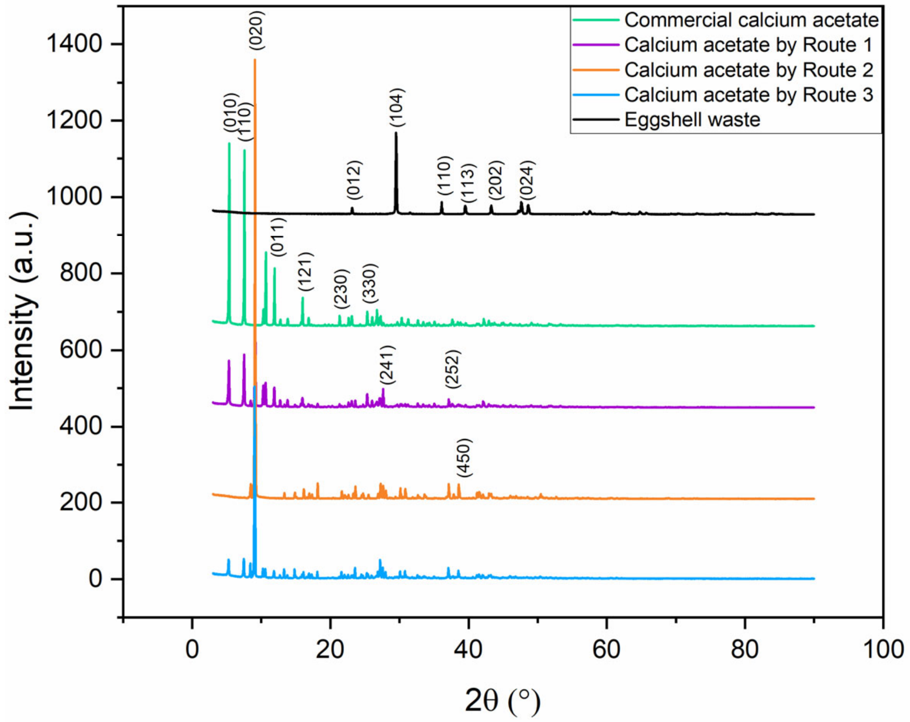

**Figure 5.** X-ray diffraction patterns of the eggshell sample, commercial calcium acetate, and calcium acetate synthesized using the three processing routes.

For the calcium acetate samples, the diffractograms revealed a distinct set of diffraction peaks, evidencing the complete conversion of calcium carbonate to calcium acetate monohydrate ($Ca(CH_3COO)_2{\cdot}H_2O$). Prominent diffraction peaks were observed at 2θ values of 5.207°, 7.394°, 9.115°, 10.602°, 11.849°, 15.957°, 21.352°, 25.419°, 27.646°, 37.047° and 38.437°, which were indexed to the crystallographic planes (010), (110), (020), (011), (012), (121), (230), (330), (241), (252) and (450), respectively.

The intense peaks observed at low angles ($2\theta < 12°$) characterize calcium acetate monohydrate and are linked to its triclinic crystal structure, which features relatively large lattice parameters and increased interplanar spacing. This structural behavior was extensively discussed by Seesanong, S. et al. [32] and Mongkol, S. et al. [33], who reported the successful synthesis of this phase from biogenic waste, such as seashells and eggshells, using aqueous solvent-assisted methods.

In addition, the absence of residual calcite peaks in the diffractograms of the calcium acetate samples indicates a high conversion efficiency during the synthesis routes employed, suggesting that the reaction conditions were adequate to promote the complete transformation of the carbonate precursor. This result is particularly relevant for biomedical applications, where the presence of secondary phases can compromise the material's reproducibility, biocompatibility, and functional performance.

In general, the XRD results confirm that eggshell waste is a viable and sustainable source of calcium for producing calcium acetate monohydrate with high crystallinity and structural purity, in agreement with previously reported studies [31–33].

The functional groups present in the raw eggshell, shell membrane, and calcium acetate samples obtained via the synthesis routes were investigated by Fourier-transform infrared spectroscopy (FTIR), as shown in Figure 6. FTIR analysis was used to confirm the chemical composition of the materials and to monitor the structural transformations associated with the conversion of calcium carbonate to calcium acetate.

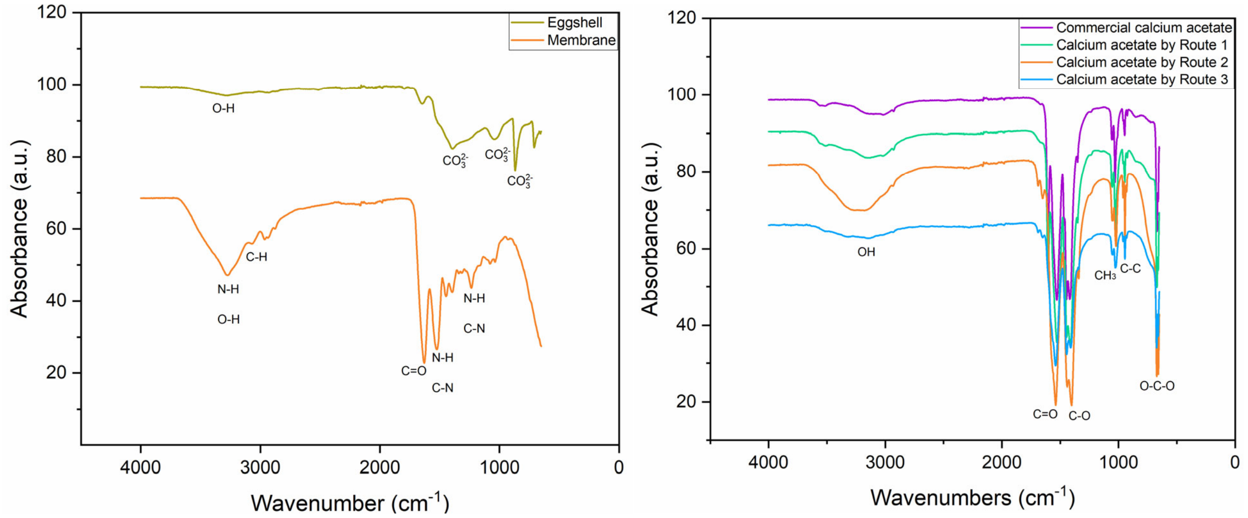

**Figure 6.** FTIR spectra of eggshell, membrane and calcium acetate samples.

The FTIR spectrum of the eggshell showed bands characteristic of calcium carbonate in the calcite phase. The intense band observed at 1391 $cm^{-1}$ is attributed to the asymmetric stretching mode $\nu_3$ of the $CO_3^{2-}$ group, typical of biogenic carbonates. The band at 1042 $cm^{-1}$ is associated with the symmetrical $\nu_1$ stretching of the carbonate ion, while the bands at 872 $cm^{-1}$ ($\nu_2$, out-of-plane bending) and 712 $cm^{-1}$ ($\nu_4$, in-plane bending) confirm the presence of the calcite crystal structure. This set of bands is widely reported in the literature for eggshells and other natural calcium carbonates, corroborating the results obtained in this study [31,34].

The spectrum of the eggshell membrane shows its predominantly organic nature. The broad band centered at 3279 $cm^{-1}$ is attributed to O–H and N–H stretching vibrations, associated with the presence of structural proteins, such as collagen, and polysaccharides. The band at 2969 $cm^{-1}$ is attributed to C–H stretching vibrations of aliphatic chains, typical of residual lipids in the membrane. Additionally, the band at 1633 $cm^{-1}$ is attributed to C=O (amide I) and C–N (amide II) stretching vibrations, characteristic of peptide bonds in proteins and glycosaminoglycans containing N-acetylglucosamine, as well as hyaluronic acid, as described by Strelec et al. [23] and other authors who investigated the biochemical composition of the eggshell membrane [24,34].

For the calcium acetate samples, the FTIR spectra showed well-defined bands at 1604 and 1530 $cm^{-1}$, attributed to the asymmetric stretching modes of the $COO^-$ group, while the bands at 1442 and 1415 $cm^{-1}$ correspond to the symmetric stretching of the same functional group. The presence of these bands confirms the formation of the carboxylate salt, in contrast to the typical carbonate vibrational modes observed in eggshell. The band at 1030 $cm^{-1}$ can be attributed to C–O stretching vibrations, while the band at 670 $cm^{-1}$ is associated with deformation vibrations of the acetate group. These results are in excellent agreement with the data reported by Strelec et al. [17], who synthesized calcium acetate from eggshell waste, as well as with additional studies involving calcium acetate monohydrate obtained from biogenic sources [32,33]. In general, FTIR spectra confirm the chemical transformation of calcium carbonate into calcium acetate, as well as the preservation of the chemical integrity of the eggshell membrane.

The chemical composition of the eggshell samples, commercial calcium acetate, and calcium acetate produced by the three synthesis routes is presented in Table 3. The results confirm that eggshells constitute a highly effective source of calcium, presenting a calcium content of 95.39%. This value is in excellent agreement with the data reported by Strelec et al. [17] and by May Yu et al. [31], who identified contents greater than 94% of $CaCO_3$ in eggshell waste from the poultry industry.

**Table 3.** Chemical composition of eggshell samples and eggshell-derived calcium acetate.

| **Composition (%)** / **Sample** | **CaO** | **MgO** | **$Na_2O$** | **$SO_3$** | **$P_2O_5$** | **$K_2O$** | **Cl** | **$SiO_2$** | **SrO** | **$Al_2O_3$** |
|---|---|---|---|---|---|---|---|---|---|---|
| Eggshell | 95.39 | 2.01 | 0.51 | 0.98 | 0.73 | - | - | 0.24 | - | 0.15 |
| Commercial calcium acetate | 99.20 | 0.60 | - | 0.20 | - | - | - | - | - | - |
| Route 1 | 90.65 | 2.67 | 1.94 | 1.85 | 1.44 | 0.62 | 0.66 | - | - | - |
| Route 2 | 93.65 | 2.66 | 1.70 | 0.75 | 0.38 | 0.41 | 0.45 | - | - | - |
| Route 3 | 94.03 | 1.56 | 1.03 | 0.77 | 1.60 | 0.53 | 0.48 | - | - | - |

The commercial calcium acetate sample, with a calcium oxide (CaO) content of 99.20%, exhibits the high purity expected for commercial-grade materials and is therefore used as a reference material to evaluate the chemical conversion and purification efficiency of the synthesis routes developed in this study. After converting calcium carbonate from eggshells to calcium acetate, all synthesized samples exhibited calcium contents of 90% or higher. This indicates a high degree of chemical conversion and an effective removal of non-calcium components. Similar results were reported by Yao et al. [18], who obtained high-purity calcium acetate from eggshells using statistical optimization of process parameters.

Among the synthesis routes evaluated, the sample obtained by Route 1 showed the lowest calcium content (90.65%), along with relatively higher levels of $Na_2O$, $SO_3$, and $P_2O_5$. This behavior suggests that Route 1 may have retained some mineral impurities and organic residues, possibly due to the use of commercial vinegar and less efficient processing conditions, including less control over reaction kinetics and less effective removal of byproducts.

In contrast, Routes 2 and 3 produced calcium acetate with calcium contents of 93.6% and 94.0%, respectively, values very close to those of commercial calcium acetate, indicating greater purification efficiency. These results suggest that the processing conditions adopted in these routes favor a more complete chemical conversion and a significant reduction in the incorporation of residual contaminants, in agreement with observations reported in the literature for reflux-assisted synthesis routes or closed systems [17,18].

The residual impurities detected at low concentrations, including MgO, $Na_2O$, $P_2O_5$, and $SiO_2$, are commonly associated with the inherent composition of eggshells and their organic membranes and have been widely reported in studies on the valorization of this biogenic residue [17,31]. The presence of these oxides in reduced concentrations is considered acceptable and does not compromise the use of the material as a precursor for biomedical or industrial applications. Overall, the high calcium content obtained—especially in Routes 2 and 3—demonstrates that the proposed synthesis routes can produce calcium acetate with a degree of purity comparable to that of commercial products. This level of purity reinforces the potential of synthesized calcium acetate as a precursor for biomaterials, bone regeneration, and other high-value-added industrial applications, while also strengthening the sustainability benefits of using waste-derived raw materials.

Thermogravimetric analysis (TGA/DTG) of eggshell and calcium acetate samples is shown in Figure 7. This analysis evaluates the thermal stability of the materials and identifies the main decomposition events associated with their chemical phases.

https://doi.org/10.3390/su18031448

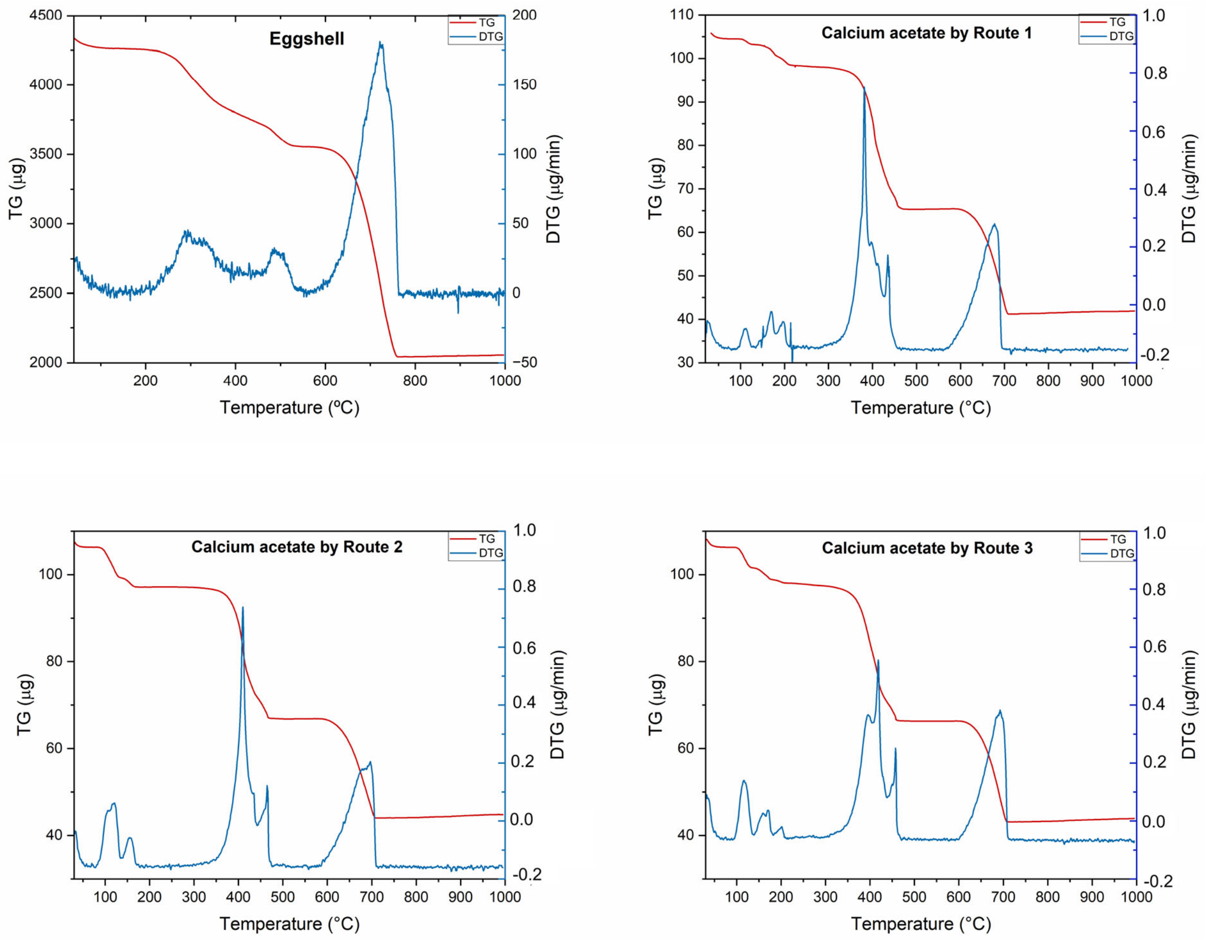

**Figure 7.** TGA/DTG curve of eggshell and calcium acetate samples obtained by different processing routes.

For the eggshell samples, an initial mass loss was observed between 40 °C and 100 °C, mainly attributed to the removal of water physically adsorbed on the surface and in the pores of the shell, as well as to water retained in the residual organic membrane. This behavior is typical of biogenic materials rich in calcium carbonate. It is in agreement with the results reported by Engin, B. et al. [34], who observed a similar event below 120 °C in chicken eggshells analyzed by TGA.

A second and main mass loss stage occurred in the range of 600 °C to 760 °C, corresponding to the thermal decomposition of calcium carbonate ($CaCO_3$) into calcium oxide (CaO), accompanied by the release of carbon dioxide ($CO_2$), according to the reaction:

$$CaCO_3 \rightarrow CaO + CO_2$$

This decomposition range is in excellent agreement with the values reported in the literature for biogenic calcium carbonates, which typically decompose between 650 °C and 800 °C, depending on crystallinity, particle size, and the presence of organic impurities [34,35]. The intensity of the corresponding peak in the DTG curve confirms that calcite is the predominant phase present in the analyzed eggshell.

In the analysis of calcium acetate samples, the TGA/DTG curves demonstrated three distinct stages of mass loss, which are characteristic of hydrated calcium acetate. The first stage, occurring up to approximately 350 °C, exhibited a mass loss of 9.4% to 10.4%. This loss is attributed to the elimination of adsorbed water and/or residual water retained after synthesis. This stage shows slight variation between the routes, indicating a similar degree of surface hydration.

The second stage occurs between 350 °C and 450 °C, with losses of 27.3–28.3%, corresponding to the decomposition of calcium acetate and the release of volatile organic species, resulting in the formation of calcium carbonate as an intermediate. The DTG curves show intense, narrow peaks in this range for all routes, suggesting that acetate decomposition occurs similarly across routes.

The third stage, observed between 600 °C and 700 °C, shows losses of 20.8–22.6%, attributed to the decomposition of $CaCO_3$ formed in the previous stage, yielding CaO. The proximity of the values indicates that all routes generate a thermally equivalent carbonate intermediate, with no significant differences in thermal stability.

The residual masses obtained range from 39.6% to 41.5%, consistent with the formation of CaO as the final decomposition product. This similarity reinforces that the three routes produce materials with essentially equivalent compositions and decomposition mechanisms. Minor numerical variations between routes may be related to subtle differences in morphology, surface area, or degree of hydration, but do not alter the overall sequence of thermal transformations.

These results show a pattern that aligns with the calcium acetate decomposition profile described by Niu et al. [35]. They identified sequential steps that involve dehydration, decomposition of the acetate group, and subsequent calcination of the intermediate carbonate. Thus, it is suggested that all routes lead to the formation of calcium acetate with comparable thermal behavior, showing that synthetic differences do not significantly impact the decomposition profile.

The morphology and surface chemical characteristics of the eggshell samples, commercial calcium acetate (control group), and calcium acetate obtained via Routes 1, 2, and 3 are presented in Figure 8. The eggshell exhibits a characteristic biogenic matrix composed of lamellae and pores distributed over an irregular surface. In the inner region of the shell, an adherent membrane composed predominantly of interwoven, coalesced fibers is observed, with a morphology consistent with that reported by Ni, and Ratner [36], and Wang et al. [37] (Figure 8a).

The commercial calcium acetate (control sample) exhibits elongated, rod-shaped particles with relatively well-defined structures, although some linear aggregation is observed (Figure 8b). In contrast, the calcium acetate obtained via Route 1 displays a highly irregular morphology, characterized by large, plate-like crystals with a broad size distribution and a strong tendency to agglomerate, hindering the identification of individual particles (Figure 8c).

The sample produced via Route 2 consists predominantly of well-defined rod-shaped particles, with a noticeably larger size than both the commercial calcium acetate and the samples obtained via Routes 1 and 3 (Figure 8d). This observation is consistent with the DLS results, which showed the highest Z-average hydrodynamic diameter for Route 2 (approximately 2775 nm), confirming a greater tendency toward particle growth and agglomeration under the employed processing conditions.

In contrast, the calcium acetate obtained via Route 3 exhibits a heterogeneous morphology, consisting of a mixture of elongated particles and irregular plate-like structures (Figure 8e). The comparatively minor and more diverse particle dimensions observed by SEM are consistent with the lower Z-average value measured by DLS for this route (approximately 2266 nm), indicating a more balanced nucleation–growth behavior and reduced agglomeration relative to Route 2.

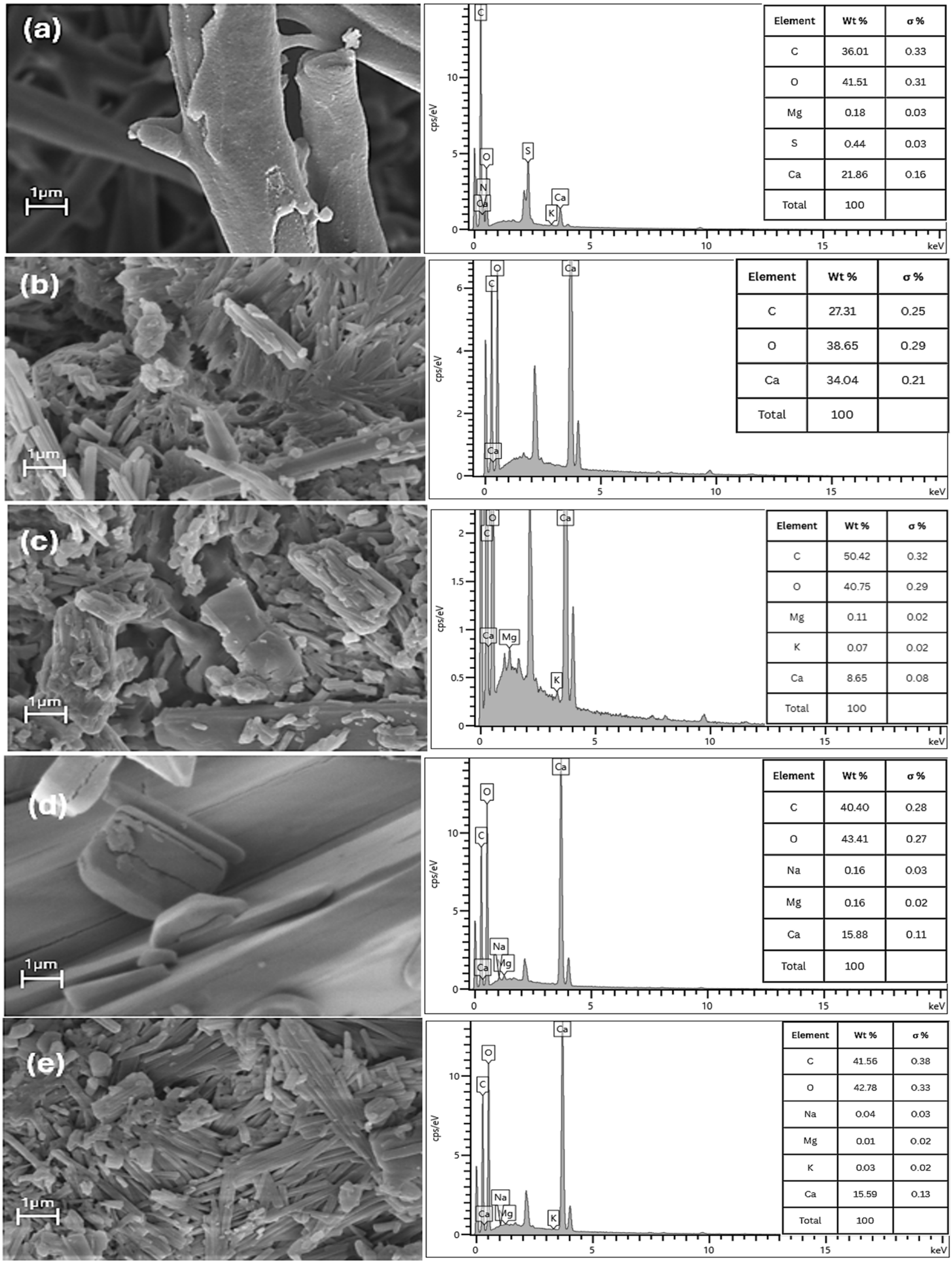

(a)

| Element | Wt % | σ % |
|---|---|---|
| C | 36.01 | 0.33 |
| O | 41.51 | 0.31 |
| Mg | 0.18 | 0.03 |
| S | 0.44 | 0.03 |
| Ca | 21.86 | 0.16 |
| Total | 100 | |

(b)

| Element | Wt % | σ % |
|---|---|---|
| C | 27.31 | 0.25 |
| O | 38.65 | 0.29 |
| Ca | 34.04 | 0.21 |
| Total | 100 | |

(c)

| Element | Wt % | σ % |
|---|---|---|
| C | 50.42 | 0.32 |
| O | 40.75 | 0.29 |
| Mg | 0.11 | 0.02 |
| K | 0.07 | 0.02 |
| Ca | 8.65 | 0.08 |
| Total | 100 | |

(d)

| Element | Wt % | σ % |
|---|---|---|
| C | 40.40 | 0.28 |
| O | 43.41 | 0.27 |
| Na | 0.16 | 0.03 |
| Mg | 0.16 | 0.02 |
| Ca | 15.88 | 0.11 |
| Total | 100 | |

(e)

| Element | Wt % | σ % |
|---|---|---|
| C | 41.56 | 0.38 |
| O | 42.78 | 0.33 |
| Na | 0.04 | 0.03 |
| Mg | 0.01 | 0.02 |
| K | 0.03 | 0.02 |
| Ca | 15.59 | 0.13 |
| Total | 100 | |

**Figure 8.** SEM micrographs and corresponding EDS spectra of samples of (**a**) eggshell, (**b**) commercial calcium acetate (control) and calcium acetate synthesized via (**c**) route 1, (**d**) route 2 and (**e**) route 3, acquired at magnification of 30 kX.

Overall, the combined SEM and DLS analyses demonstrate that the synthesis route strongly influences particle size and agglomeration behavior. Route 2 promotes the formation of larger calcium acetate particles, whereas Route 3 yields comparatively finer and more heterogeneous structures, and Route 1 results in poorly defined, highly agglomerated morphologies.

The EDS analysis (Figure 8) confirms the differences observed in the microstructure. The analysis indicates that eggshells are primarily made up of oxygen (41.51%), carbon (36.01%), and calcium (21.86%), which aligns with their main component, calcium carbonate ($CaCO_3$). Calcium acetate samples, derived from processed eggshells, display elements characteristic of calcium acetate, along with small amounts of magnesium, sodium, and potassium, as shown in the X-ray fluorescence results. These impurities occur due to the variable composition of eggshells, even though they are predominantly composed of calcium carbonate.

XPS analyses of calcium acetate samples obtained by the three synthesis routes are presented in Figures 9–11. This technique was employed to assess the presence of residual organic groups, the chemical state of calcium, and surface impurities, which included sodium (Na), magnesium (Mg), chlorine (Cl), and nitrogen (N).

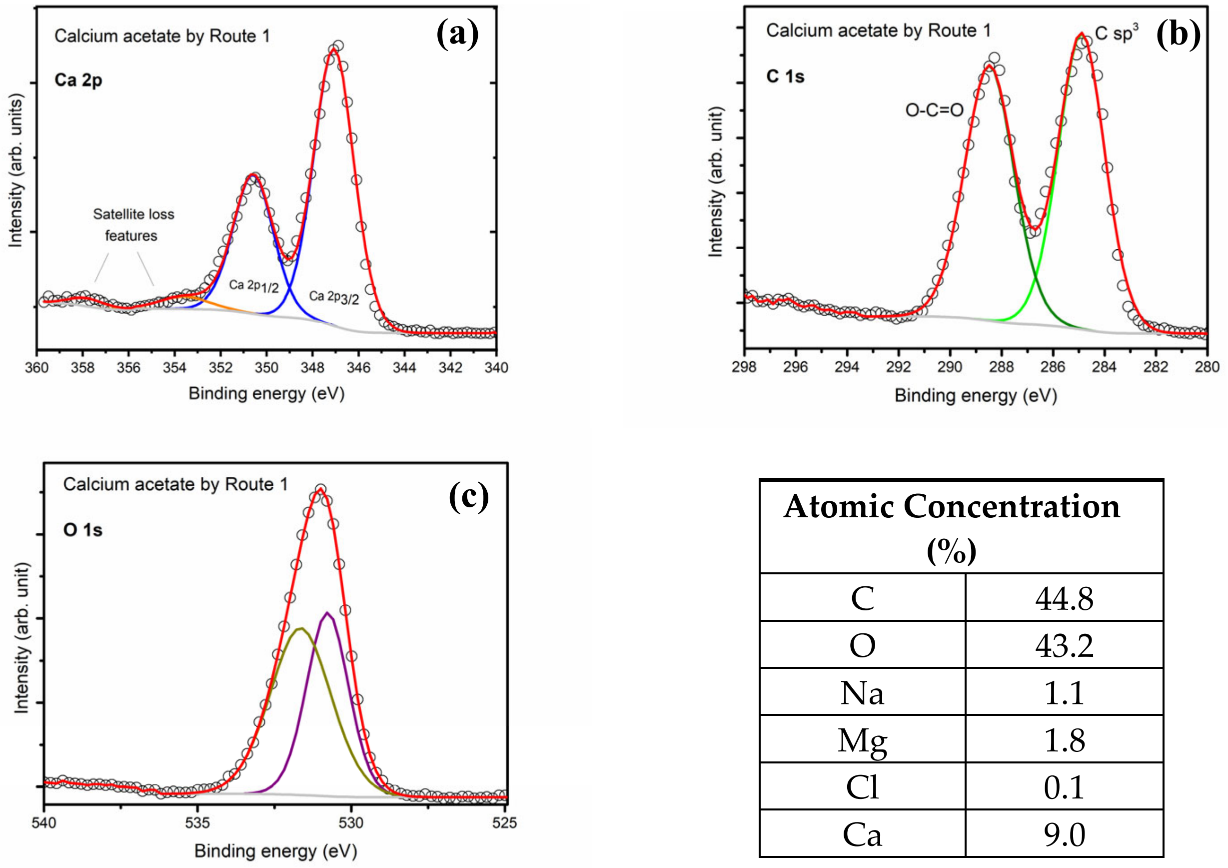

| Atomic Concentration (%) | |
|---|---|
| C | 44.8 |
| O | 43.2 |
| Na | 1.1 |
| Mg | 1.8 |
| Cl | 0.1 |
| Ca | 9.0 |

**Figure 9.** X-ray photoelectron spectroscopy (XPS) spectra of calcium acetate by route 1 for the regions (**a**) Ca 1s, (**b**) C 1s, and (**c**) O 1s. The O 1s envelope was fitted with two components centered at (i) 530.8 eV for the oxygen BE from OH–groups as well as $(CO_3)^{2-}$ adsorbed on the surface; (ii) 532.2 eV, attributed to oxygens of adsorbed water on the surface. Open dots experimental data. Red line result of the fitting procedure. Gray line background. XPS spectra acquired with a pass energy of 27 eV and an analysis area of 200 × 200 μm$^2$.

https://doi.org/10.3390/su18031448

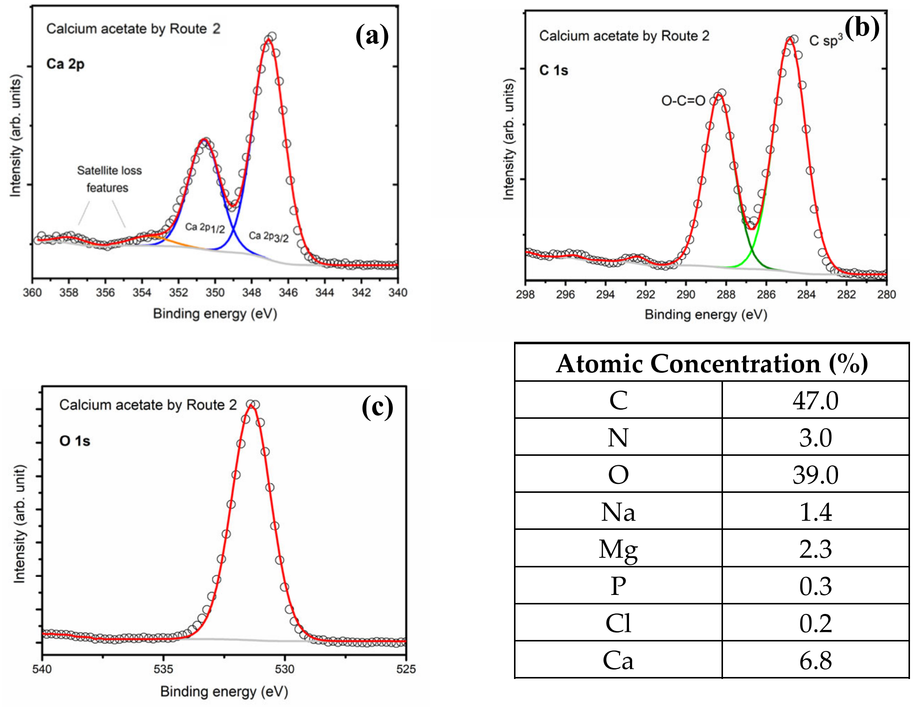

| Atomic Concentration (%) | |
|---|---|
| C | 47.0 |
| N | 3.0 |
| O | 39.0 |
| Na | 1.4 |
| Mg | 2.3 |
| P | 0.3 |
| Cl | 0.2 |
| Ca | 6.8 |

**Figure 10.** X-ray photoelectron spectroscopy (XPS) spectra of calcium acetate by route 2 for the regions (**a**) Ca 1s, (**b**) C 1s, and (**c**) O 1s. The O 1s envelope was fitted with one component centered at 530.8 eV for OH–groups as well as $(CO_3)^{2-}$ adsorbed on the surface. Open dots experimental data. Red line result of the fitting procedure. Gray line background. XPS spectra acquired with a pass energy of 27 eV over an area of 200 × 200 μm$^2$.

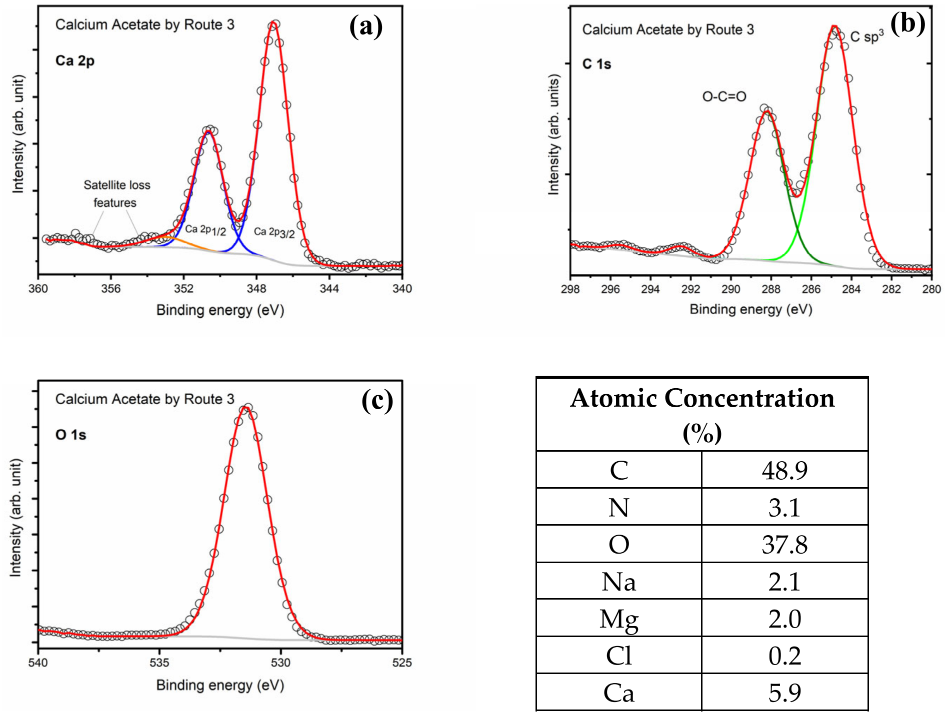

| Atomic Concentration (%) | |
|---|---|
| C | 48.9 |
| N | 3.1 |
| O | 37.8 |
| Na | 2.1 |
| Mg | 2.0 |
| Cl | 0.2 |
| Ca | 5.9 |

**Figure 11.** X-ray photoelectron spectroscopy (XPS) spectra of calcium acetate by route 3 for the regions (**a**) Ca 1s, (**b**) C 1s, and (**c**) O 1s. The O 1s envelope was fitted with one component centered at 530.8 eV for OH–groups as well as $(CO_3)^{2-}$ adsorbed on the surface. Open dots experimental data. Red line result of the fitting procedure. Gray line background. XPS spectra acquired with a pass energy of 27 eV over an area of 200 × 200 μm$^2$.

The calcium acetate sample obtained via processing Route 1 exhibited a higher surface calcium concentration compared to those produced by Routes 2 and 3, as revealed by XPS analysis. This result suggests that Route 1 promotes an efficient surface-level conversion of eggshell-derived calcium carbonate into calcium-containing species. However, the simultaneously higher surface concentrations of carbon and oxygen indicate a predominance of adsorbed and hydrated calcium acetate species (Figure 9). This finding implies that, although Route 1 enhances surface calcium exposure, it also favors the retention of hydration layers and organic residues, which may be associated with less effective purification during processing [38].

In contrast, the samples obtained via Routes 2 and 3 exhibited lower surface concentrations of carbon and oxygen, together with reduced levels of residual elements such as Na, Mg, and Cl (Figures 9–11). These elements are commonly associated with the intrinsic composition of eggshells and their organic membrane [39,40]. Their lower surface abundance suggests that Routes 2 and 3 promote a more homogeneous chemical conversion and improved impurity removal, resulting in cleaner calcium acetate surfaces. This observation is consistent with the higher bulk calcium levels determined by chemical analysis and indicates that these routes are more effective in achieving overall product purity.

Although the chemical shifts observed in the Ca 2p XPS spectra of the calcium acetate samples are relatively small, careful peak deconvolution reveals the coexistence of calcium in multiple chemical environments. One contribution corresponds to calcium coordinated to carboxylate oxygens, characteristic of acetate formation, while additional components are associated with carbonate remnants or hydrated calcium species. This multiplicity of chemical states corroborates the results obtained by XRD, FTIR, and TGA/DTG, which collectively indicate that the synthesized products are predominantly hydrated calcium acetates.

The Ca 2p binding energies observed for the synthesized samples are close to those reported for both calcium carbonate and calcium acetate, reflecting the similar electronic environments of $Ca^{2+}$ in these compounds. Nevertheless, subtle variations in binding energy and peak asymmetry (Figures 9a, 10a and 11a) can be attributed to differences in local coordination and surface hydration, which are directly influenced by the processing route employed.

The C 1s spectra further support these interpretations. The component centered at approximately 289 eV, together with additional contributions, is characteristic of carboxylate groups (O–C=O), confirming the presence of acetate species chemically bound to calcium. Meanwhile, peaks observed between 285 and 286 eV correspond to the methyl group ($–CH_3$) of the acetate molecule (Figures 9b, 10b and 11b) [41]. The relative intensities of these components are higher for Route 1, reinforcing the conclusion that this route leads to a greater amount of surface-adsorbed organic species, whereas Routes 2 and 3 yield more chemically stable, less hydrated surfaces.

Overall, the XPS results demonstrate that while Route 1 favors rapid surface conversion, it is less effective in limiting surface hydration and residual organics. In contrast, Routes 2 and 3 provide a more balanced combination of efficient chemical conversion, reduced impurity retention, and improved surface purity. Route 3 offers the best compromise between conversion efficiency and surface chemical stability, making it the most successful processing route for producing calcium acetate from eggshell waste.

## 4. Conclusions

The large-scale disposal of eggshells poses a significant environmental and economic challenge, as this agro-industrial waste is generated in large volumes and is often inadequately managed. The present study aimed to investigate and compare three processing routes for converting eggshell waste into hydrated calcium acetate, evaluating their technical efficiency and potential applicability.

Among the methodologies evaluated, Route 3 emerged as the most promising alternative, offering the shortest processing time and maintaining a byproduct yield comparable to that of the other routes. Chemical and thermal analyses confirmed the quality of the materials obtained in all routes, reinforcing the viability of transforming eggshell waste into a valuable calcium precursor with potential for industrial and biomedical applications.

Despite these positive results, some limitations should be considered. The use of commercial vinegar as a source of acetic acid may influence the reproducibility and control of the final product composition. Furthermore, the natural variability in eggshell characteristics and the colloidal instability observed in calcium acetate particles represent additional challenges. Issues related to process scalability, reproducibility when using different waste sources, and the risks associated with organic contamination also require careful evaluation.

Therefore, future studies should focus on improving particle stability, standardizing raw materials, replacing or regulating the acid source, and evaluating the material's performance in specific biomedical applications. Furthermore, comprehensive technical and economic feasibility analyses at an industrial scale will be essential to consolidate the potential of the proposed processing routes as a sustainable solution for the valorization of eggshell waste.

**Author Contributions:** Conceptualization, J.K.d.O.S., C.B., A.Z.S. and A.P.R.A.; Methodology, J.K.d.O.S., C.B., A.Z.S. and A.P.R.A.; Validation, J.K.d.O.S., C.B., A.Z.S. and A.P.R.A.; Formal analysis, J.K.d.O.S. and C.B.; Investigation, J.K.d.O.S.; Writing—review & editing, J.K.d.O.S., C.B., A.Z.S. and A.P.R.A.; Visualization, J.K.d.O.S., C.B. and A.P.R.A.; Supervision, A.Z.S. and A.P.R.A. All authors have read and agreed to the published version of the manuscript.

**Funding:** This work was supported financially by the São Paulo Research Foundation (FAPESP), through research grants No. 2024/04829-4, No. 2022/14790-2 (NWO) and No. 2024/11110-6 (WBI), and from the National Council for Scientific and Technological Development (CNPq), project No. 445151/2024-2.

**Institutional Review Board Statement:** Not applicable.

**Informed Consent Statement:** Not applicable.

**Data Availability Statement:** The original contributions presented in this study are included in the article. Further inquiries can be directed to the corresponding author.

**Acknowledgments:** The authors would like to thank the Guaratinguetá School of Engineering and Sciences–UNESP (São Paulo State University) and the Institute for Research in Materials Science and Engineering at the University of Mons for their institutional support and the infrastructure provided. They would also like to thank the laboratories involved for their technical assistance and support during the execution of this work.

**Conflicts of Interest:** The authors declare no conflict of interest.

## References

1. FAO. *Gateway to Poultry Production and Products*; FAO: Rome, Italy, 2025.
2. Pagonis, N.; Flegkas, D.; Itziou, A.; Kountouras, K.; Stimoniaris, A.; Samaras, P.; Karayannis, V. Upcycling of eggshell waste into calcium phosphates for use in sustainable biomedical engineering applications. *Eng* **2024**, *5*, 3540–3550. [CrossRef]
3. Torres Gouveia, M.E.; Milhans, C.; Gezek, M.; Camci-Unal, G. Eggshell-based unconventional biomaterials for medical applications. *Adv. NanoBiomed Res.* **2025**, *5*, 2400120. [CrossRef]
4. Kumar, T.S.S.; Madhumathi, K.; Jayasree, R. Eggshell waste: A gold mine for sustainable bioceramics. *J. Indian Inst. Sci.* **2022**, *102*, 599–620. [CrossRef]
5. Hembrick-Holloman, V.; Samuel, T.; Mohammed, Z.; Jeelani, S.; Rangari, V.K. Ecofriendly production of bioactive tissue engineering scaffolds derived from egg- and seashells. *J. Mater. Res. Technol.* **2020**, *9*, 13729–13739. [CrossRef]

6. Huang, K.; Hou, J.; Gu, Z.; Wu, J. Egg-white/eggshell-based biomimetic hybrid hydrogels for bone regeneration. *ACS Biomater. Sci. Eng.* **2019**, *5*, 5384–5391. [CrossRef] [PubMed]
7. Tavangar, A.; Tan, B.; Venkatakrishnan, K. Synthesis of three-dimensional calcium carbonate nanofibrous structure from eggshell using femtosecond laser ablation. *J. Nanobiotechnol.* **2011**, *9*, 1. [CrossRef]
8. Torres-Mansilla, A.; Álvarez-Lloret, P.; Fernández-Penas, R.; D'Urso, A.; Baldión, P.A.; Oltolina, F.; Follenzi, A.; Gómez-Morales, J. Hydrothermal transformation of eggshell calcium carbonate into apatite micro-nanoparticles: Cytocompatibility and osteoinductive properties. *Nanomaterials* **2023**, *13*, 2299. [CrossRef]
9. Habte, L.; Shiferaw, N.; Mulatu, D.; Thenepalli, T.; Chilakala, R.; Ahn, J.W. Synthesis of nano-calcium oxide from waste eggshell by sol–gel method. *Sustainability* **2019**, *11*, 3196. [CrossRef]
10. Adaikalam, K.; Hussain, S.; Anbu, P.; Rajaram, A.; Sivanesan, I.; Kim, H.-S. Eco-friendly facile conversion of waste eggshells into CaO nanoparticles for environmental applications. *Nanomaterials* **2024**, *14*, 1620. [CrossRef]
11. Ahmed, T.A.; Wu, L.; Younes, M.; Hincke, M. Biotechnological applications of eggshell: Recent advances. *Front. Bioeng. Biotechnol.* **2021**, *9*, 675364. [CrossRef] [PubMed]
12. Afrrin, M.; Rajasekaran, B.; Nandhini, R.S.; Karthik, P. Valorization of eggshell waste for sustainable food packaging: A review. *Food Bioprocess Technol.* **2025**, *18*, 10209–10228. [CrossRef]
13. Nada, E.A.; Abu Kaddorah, M.E.; El Jamal, M.; Hamad, A.; Mansour, F.R. Eggshell waste as a sustainable resource for nanoparticle preparation: Synthesis, characterization and applications. *Environ. Nanotechnol. Monit. Manag.* **2025**, *24*, 101092. [CrossRef]
14. Baláž, M.; Boldyreva, E.V.; Rybin, D.; Pavlović, S.; Mudrinić, T.; Luque, R. State-of-the-art of eggshell waste in materials science: Recent advances in catalysis, pharmaceutical applications, and mechanochemistry. *Front. Bioeng. Biotechnol.* **2021**, *8*, 612567. [CrossRef]
15. Heo, W.; Shin, H.; Ansari, J.R.; Park, K.; Seo, J. Preparation and properties of calcium oxide and calcium peroxide from eggshell waste for enhanced antimicrobial activity. *Mater. Today Commun.* **2024**, *41*, 110531. [CrossRef]
16. Bhuvaneshwari, V.; Sonia, S.; Sivaganesh, D. Harnessing the potency of eco-friendly calcium oxide derived from eggshells for enhanced photocatalytic activity and biocompatibility evaluation in HepG2 cell line. *Chem. Phys. Impact* **2024**, *9*, 100699. [CrossRef]
17. Strelec, I.; Tomičić, K.; Zajec, M.; Ostojčić, M.; Budžaki, S. Eggshell-waste-derived calcium acetate, calcium hydrogen phosphate and corresponding eggshell membranes. *Appl. Sci.* **2023**, *13*, 7372. [CrossRef]
18. Yao, Y.; Wang, L.; Zhang, Y.; Liu, H. Optimization of preparation of calcium acetate from eggshell by response surface methodology. *Food Sci. Technol.* **2022**, *42*, e10221. [CrossRef]
19. Menglieva, S.; Khozhiev, S.; Usmanova, Z.; Tukhtaev, K. The technology of green synthesis of calcium acetate from quail eggshells. *BIO Web Conf.* **2024**, *82*, 04001. [CrossRef]
20. Ningrum, R.A.; Humaidi, S.; Sihotang, S.; Bonardo, D.; Estananto. Synthesis and material characterization of calcium carbonate ($CaCO_3$) from the waste of chicken eggshells. *J. Phys. Conf. Ser.* **2022**, *2193*, 012009. [CrossRef]
21. Zia, J.; Shringi, A.K.; Riaz, U. Calcium oxide nanoparticles from eggshell waste: A green nanotechnological strategy for microwave-assisted environmental cleanup. *Clean. Chem. Eng.* **2025**, *11*, 100182. [CrossRef]
22. Rivera, E.M.; Araiza, M.; Brostow, W.; Castaño, V.M.; Díaz-Estrada, J.R.; Hernández, R.; Rodríguez, J.R. Synthesis of hydroxyapatite from eggshells. *Mater. Lett.* **1999**, *41*, 128–134. [CrossRef]
23. Strelec, I.; Ostojčić, M.; Brekalo, M.; Hajra, S.; Kim, H.-J.; Stanojev, J.; Maravić, N.; Budžaki, S. Transformation of eggshell waste to egg white protein solution, calcium chloride dihydrate, and eggshell membrane powder. *Green Process. Synth.* **2023**, *12*, 20228151. [CrossRef]
24. Torres-Mansilla, A.; Hincke, M.; Voltes, A.; López-Ruiz, E.; Baldión, P.A.; Marchal, J.A.; Álvarez-Lloret, P.; Gómez-Morales, J. Eggshell membrane as a biomaterial for bone regeneration. *Polymers* **2023**, *15*, 1342. [CrossRef]
25. Honary, S.; Zahir, F. Effect of zeta potential on the properties of nano-drug delivery systems—A review. *Trop. J. Pharm. Res.* **2013**, *12*, 255–264. [CrossRef]
26. Bhattacharjee, S. DLS and zeta potential—What they are and what they are not. *J. Control. Release* **2016**, *235*, 337–351. [CrossRef]
27. Vo, Q.C.; Son, G.; Seon, G.M.; Um, S.W.; Choi, S.H.; Yang, H.-C. Effect of nanoparticulate $CaCO_3$ on the biological properties of calcium silicate cement. *Sci. Rep.* **2025**, *15*, 478. [CrossRef]
28. Dorozhkin, S.V. Bioceramics of calcium orthophosphates. *Biomaterials* **2010**, *31*, 1465–1485. [CrossRef]
29. Min, K.H.; Kim, D.H.; Kim, K.H.; Seo, J.-H.; Pack, S.P. Biomimetic scaffolds of calcium-based materials for bone regeneration. *Biomimetics* **2024**, *9*, 511. [CrossRef] [PubMed]
30. Li, C.-Q.; Liang, C.; Chen, Z.-M.; Di, Y.-H.; Zheng, S.-L.; Wei, S.; Sun, Z.-M. Surface modification of calcium carbonate: A review of theories, methods and applications. *J. Cent. South Univ.* **2021**, *28*, 2589–2611. [CrossRef]
31. May, Y.; Nyein, O.M.; Kha, N.N. Comparative study on the characteristics of eggshell wastes for preparation of calcium acetate. *J. Myanmar Acad. Arts Sci.* **2019**, *17*, 335–354.

32. Seesanong, S.; Seangarun, C.; Boonchom, B.; Ohpasee, N.; Laohavisuti, N.; Boonmee, W.; Rungrojchaipon, P. Green Ca-source of cockle shells converted to calcium acetate for environmental sustainability. *Heliyon* **2024**, *10*, e32153. [CrossRef] [PubMed]
33. Mongkol, S.; Seesanong, S.; Boonchom, B.; Laohavisuti, N.; Boonmee, W.; Thompho, S.; Rungrojchaipon, P. Simple rapid production of calcium acetate lactate from scallop shell waste for agricultural application. *Int. J. Mol. Sci.* **2025**, *26*, 4488. [CrossRef]
34. Engin, B.; Demirtaş, H.; Eken, M. Temperature effects on eggshells investigated by XRD, IR and ESR techniques. *Radiat. Phys. Chem.* **2006**, *75*, 268–277. [CrossRef]
35. Niu, S.; Han, K.; Lu, C.; Sun, R. Thermogravimetric analysis of the relationship among calcium magnesium acetate, calcium acetate and magnesium acetate. *Appl. Energy* **2010**, *87*, 2237–2242. [CrossRef]
36. Ni, M.; Ratner, B.D. Differentiating calcium carbonate polymorphs by surface analysis techniques—An XPS and TOF-SIMS study. *Surf. Interface Anal.* **2008**, *40*, 1356–1361. [CrossRef]
37. Wang, Q.; Jiang, Z.; Wang, Y.; Chen, D.; Yang, D. Photocatalytic properties of porous C-doped $TiO_2$ and Ag/C-doped $TiO_2$ nanomaterials by eggshell membrane templating. *J. Nanopart. Res.* **2009**, *11*, 375–384. [CrossRef]
38. Garduño-Pineda, L.; Linares-Hernández, I.; Solache-Ríos, M.J.; Teutli-Sequeira, A.; Martínez-Miranda, V. Removal of inorganic chemical species and organic matter from slaughterhouse wastewater via calcium acetate synthesized from eggshell. *J. Environ. Sci. Health A* **2019**, *54*, 295–305. [CrossRef] [PubMed]
39. Minakshi, M.; Higley, S.; Baur, C.; Mitchell, D.R.G.; Jones, R.T.; Fichtner, M. Calcined chicken eggshell electrode for battery and supercapacitor applications. *RSC Adv.* **2019**, *9*, 26981–26995. [CrossRef]
40. Thermo Fisher Scientific. *Calcium and Carbon XPS Reference Binding Energies*; Thermo Fisher Scientific: Waltham, MA, USA; Available online: https://www.thermofisher.com/th/en/home/materials-science/learning-center/periodic-table/non-metal/carbon.html (accessed on 7 November 2025).
41. Mudiyanselage, K.; Burrell, A.; Senanayake, S.; Idriss, H. XPS and NEXAFS study of the reactions of acetic acid and acetaldehyde over $UO_2$(100) thin film. *Surf. Sci.* **2019**, *680*, 107–112. [CrossRef]